Complete Characterization of Transmission Losses in Generalized Nonradiative Dielectric (NRD) Waveguide

Jean Dallaire, *Member, IEEE,* and Ke Wu, *Senior Member, IEEE*

***Abstract*—In this paper, transmission losses of the generalized nonradiative dielectric (NRD) waveguide are modeled and presented by our closed-form equations for the design of hybrid and monolithic millimeter-wave integrated circuits. This generalized structure includes our recently proposed channelized NRD-guide. Parametric effects are studied with respect to complex propagation constant and characteristic impedance, and some useful guidelines are generated for practical design considerations. Calculated results are discussed separately for the conductor and dielectric losses for the two fundamental longitudinal section electric (LSE) and longitudinal section magnetic (LSM) modes. It is found that the LSE mode may have losses, in some cases, comparable or even smaller than those of its LSM counterpart, contradicting what has usually been perceived for the conventional NRD-guide design.**

***Index Terms*—Closed-form equations, generalized nonradiative dielectric waveguide, LSE mode, LSM mode, microwave, millimeter wave, theoretical complex propagation constant.**

I. Introduction

THE nonradiative dielectric waveguide (NRD-guide) was first introduced by Yoneyama [1] with the aim of creating a low-loss transmission line at millimeter-wave frequencies. The NRD-guide is quite similar to the H-guide in topology, but its guided modes are nonradiating even in the presence of sharp bends and discontinuities. Such a desirable feature is attributed to the fact that the NRD-guide operates under the inherent cutoff frequency of the parallel-plate TE and TM modes, making the NRD-guide very attractive for millimeter-wave applications. Very recently, a new NRD-guide, i.e., channelized NRD-guide, was proposed in [2] and [3], which consists of a core dielectric strip surrounded by dielectric materials having a relatively lower dielectric constant (the outer region). In this way, the generalized structure, as shown in Fig. 1, retains all of the advantages of an NRD-guide, whereas the spacing of the two metallic plates is proportionally reduced with respect to the square root of the outer dielectric constant. In addition, such a reduced spacing at millimeter-wave frequencies may fit with a thickness of semiconductor wafer, which can be used to design a monolithically integrated NRD-guide completely compatible with monolithic-microwave integrated-circuit (MMIC) design.

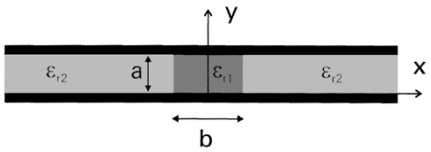

Fig. 1. Configuration of the general NRD circuit.

To characterize electrical properties of the generalized NRD-guide, transmission loss due to its imperfect metallic plates and dielectric regions should be considered as a predominant factor together with other parameters, namely, propagation constant and characteristic impedance. The transmission loss of the fundamental longitudinal section magnetic (LSM) mode in an NRD-guide is usually perceived lower than that of its longitudinal section electric (LSE) counterpart. This is why the LSM mode is preferred over the LSE mode. However, it is found by modeling the new structure that, in some cases, the transmission loss of the LSE mode is comparable and even lower than that of the LSM mode. Therefore, an adequate choice for the fundamental mode is revoked.

On the other hand, it is interesting to give a fresh look into the advantages of using the nonradiating LSE_{10} mode that has the lowest cutoff frequency. First of all, there is no need for a mode suppressor [4] since the NRD becomes an LSE_{10} monomode transmission line. Further, the LSE_{10} mode may provide a larger frequency bandwidth than the LSM_{10} mode does. Similar to the use of the LSM mode, the LSE-mode baluns can also be designed for the hybrid integration technology of planar circuits and NRD-guides [5], [6]. In this paper, a comparative study of the two modes and their design features are presented for the proposed generalized NRD-guide with emphasis on the transmission loss.

II. Transmission Loss and Propagation Constant

Since the materials used to build an NRD-guide usually have a low-loss property ($\sigma \approx 10^7 - 10^8$ S/m for the metallic plates and $\tan\delta \approx 10^{-3} - 10^{-4}$ for dielectrics at millimeter-wave frequencies), a perturbation method is used to calculate the transmission losses. In this method, we assume that the electromagnetic field calculated for the perfect guide is similar to the perturbed field of the lossy guide. The attenuation constant is then

Manuscript received April 22, 1999. This work was supported by the Natural Sciences and Engineering Research Council of Canada and by the Fonds pour la Formation de Chercheurs et l'Aide à la Recherche.

J. Dallaire was with the Departement de Génie Électrique et de Génie Informatique, Poly-Grames Research Center, École Polytechnique de Montréal, Montréal, P.Q., Canada H3C 3A7. He is now with EMS Technologies Canada, P.Q., Canada H9X 3R2.

K. Wu is with the Departement de Génie Électrique et de Génie Informatique, Poly-Grames Research Center, École Polytechnique de Montréal, Montréal, P.Q., Canada H3C 3A7.

Publisher Item Identifier S 0018-9480(00)00224-6.

calculated from the unperturbed field of the perfect guide. In view of the generalized structure depicted in Fig. 1, the separation of the parallel plates denoted by "a" should be less than half of the guided-wavelength of a TEM mode in the outer dielectric region. This condition is simply $a < \lambda/2$, which could also be written for the maximum permissible frequency

$$f < c/2a\sqrt{\epsilon_{r2}}. \tag{1}$$

As indicated above, the calculation of transmission loss begins with the formulation of the fields in the lossless structure. Details of the analytical procedure can be found in [7]. The characteristic equations for the two classes of mode are given as follows:

LSM:

$$\text{even:} \quad k_{y1}\tan\left(\frac{k_{y1}b}{2}\right) = \left(\frac{\varepsilon_{r1}}{\varepsilon_{r2}}\right)k_{y2}$$

$$\text{odd:} \quad k_{y1}\cot\left(\frac{k_{y1}b}{2}\right) = -\left(\frac{\varepsilon_{r1}}{\varepsilon_{r2}}\right)k_{y2}$$

LSE:

$$\text{even:} \quad k_{y1}\tan\left(\frac{k_{y1}b}{2}\right) = k_{y2}$$

$$\text{odd:} \quad k_{y1}\cot\left(\frac{k_{y1}b}{2}\right) = -k_{y2}.$$

The propagation constant is simply defined as $\beta = \sqrt{\varepsilon_{r1}k_0^2 - k_x^2 - k_{y1}^2} = \sqrt{\varepsilon_{r2}k_0^2 - k_x^2 + k_{y2}^2}$ where k_{y1} and k_{y2} are, respectively, the propagation and attenuation constants in the core and outer dielectric regions, $k_x = m\pi/a$ and $k_0 = \omega/c$. The loss calculation due to imperfect conductors by the perturbation method [7] can be made by

$$\alpha_c = \frac{P_c/l}{2P} \tag{2}$$

where P_c/l is the power dissipated in the metallic plates per unit length and P is the total power flow. This can be calculated by

$$\begin{aligned} P_c/l &= \left(\frac{1}{2}R_s I^2\right)/l \\ &= 2R_s\left\{\int_0^{b/2}\left(\vec{J}_1\cdot\vec{J}_1^*\right)dy + \int_{b/2}^{\infty}\left(\vec{J}_2\cdot\vec{J}_2^*\right)dy\right\} \end{aligned} \tag{3}$$

where $\vec{J}_1 = \hat{n}\times\vec{H}_1$ and $\vec{J}_2 = \hat{n}\times\vec{H}_2$ are the surface current densities on one metal plate in regions I and II. $R_S = \sqrt{\omega\mu_0/2\sigma}$ is the surface resistance of the metal plates. The power flow for the LSM mode, called $P(\text{LSM})$, is

$$\begin{aligned} P(\text{LSM}) &= \int_{-\infty}^{+\infty}\int_0^a \frac{1}{2}\text{Re}\left(\vec{E}\times\vec{H}^*\right)\cdot\hat{z}\,dx\,dy \\ &= -\int_{-\infty}^{+\infty}\int_0^a E_y H_x^*\,dx\,dy \end{aligned} \tag{4}$$

while the power flow for the LSE mode, called $P(\text{LSE})$, is

$$P(\text{LSE}) = \int_{-\infty}^{+\infty}\int_0^a E_x H_y^*\,dx\,dy. \tag{5}$$

As such, the resulting transmission losses are analytically found from

$$\alpha_c\,(\text{LSM}_{\text{EVEN}}) = \frac{2R_S}{aZ_0^M}\left(\frac{k_x}{\beta}\right)^2\left(\frac{N_1}{D_1}\right) \tag{6}$$

$$\alpha_c\,(\text{LSM}_{\text{ODD}}) = \frac{2R_S}{aZ_0^M}\left(\frac{k_x}{\beta}\right)^2\left(\frac{N_2}{D_2}\right) \tag{7}$$

$$\alpha_c\,(\text{LSE}_{\text{EVEN}}) = \frac{2R_S}{aZ_0^E}\left(\frac{\beta^2 b k_{y1}^3}{(\beta^2+k_x^2)^2 D_1} + 1\right) \tag{8}$$

$$\alpha_c\,(\text{LSE}_{\text{ODD}}) = \frac{2R_S}{aZ_0^E}\left(\frac{-\beta^2 b k_{y1}^3}{(\beta^2+k_x^2)^2 D_2} - 1\right) \tag{9}$$

where

$$\begin{aligned} N_1 &= bk_{y1} + \sin\,(bk_{y1})\left\{1 + (\varepsilon_{r2}/\varepsilon_{r1})\,(k_{y1}/k_{y2})^2\right\} \\ N_2 &= -bk_{y1} + \sin\,(bk_{y1})\left\{1 + (\varepsilon_{r2}/\varepsilon_{r1})\,(k_{y1}/k_{y2})^2\right\} \\ D_1 &= bk_{y1} + \sin\,(bk_{y1})\left\{1 + (k_{y1}/k_{y2})^2\right\} \\ D_2 &= bk_{y1} - \sin\,(bk_{y1})\left\{1 + (k_{y1}/k_{y2})^2\right\} \\ Z_0^M &= \frac{\beta^2 + k_x^2}{\beta\omega\varepsilon} \\ Z_0^E &= \frac{\beta\omega\mu}{\beta^2 + k_x^2}. \end{aligned}$$

Similarly, the transmission loss due to imperfect dielectric materials is also calculated by a perturbation method [7] as follows:

$$\alpha_d = \frac{P_d/l}{2P} \tag{10}$$

where P_d/l is the power dissipated in the dielectric materials per unit length, which can easily be obtained by

$$\begin{aligned} P_d/l = {} & \omega\varepsilon_1\tan\,\delta_1\int_0^{b/2}\int_0^a \left|\vec{E}_1\right|^2 dx\,dy \\ & + \omega\varepsilon_2\tan\,\delta_2\int_0^{b/2}\int_0^a \left|\vec{E}_2\right|^2 dx\,dy. \end{aligned} \tag{11}$$

Therefore, the resulting dielectric losses for the two groups of modes are formulated by

$$\alpha_d\,(\text{LSM}_{\text{EVEN}}) = \frac{\varepsilon_{r1}k_o^2\tan\,\delta_1}{2\beta}\cdot\frac{N_3}{D_1} + \frac{\varepsilon_{r2}k_o^2\tan\,\delta_2}{2\beta}\cdot\frac{N_5}{D_1} \tag{12}$$

$$\alpha_d\,(\text{LSM}_{\text{ODD}}) = \frac{\varepsilon_{r1}k_o^2\tan\,\delta_1}{2\beta}\cdot\frac{N_4}{D_2} + \frac{\varepsilon_{r2}k_o^2\tan\,\delta_2}{2\beta}\cdot\frac{N_5}{D_2} \tag{13}$$

$$\begin{aligned} \alpha_d\,(\text{LSE}_{\text{EVEN}}) = {} & \frac{\varepsilon_{r1}k_o^2\tan\,\delta_1}{2\beta}\cdot\frac{bk_{y1} + \sin\,(bk_{y1})}{D_1} \\ & + \frac{\varepsilon_{r2}k_o^2\tan\,\delta_2}{2\beta}\cdot\frac{\sin\,(bk_{y1})\,(k_{y1}/k_{y2})^2}{D_1} \end{aligned} \tag{14}$$

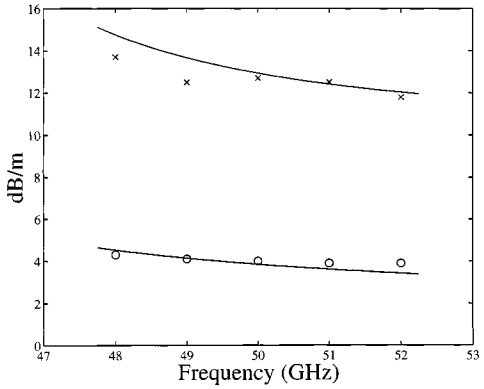

Fig. 2. Total transmission losses for LSM_{10}, measured [8] (X: polystyrene, O: Teflon) and calculated by (6) and (12). Polystyrene: $a = 2.7$ mm, $b = 2.4$ mm, $\varepsilon_{r1} = 2.56$, $\tan\delta_1 = 9 \times 10^{-4}$. Teflon: $a = 2.85$ mm, $b = 3.2$ mm, $\varepsilon_{r2} = 2.04$, $\tan\delta_2 = 1.5 \times 10^{-4}$. Region II is vacuum.

$$\alpha_d(\mathrm{LSE_{ODD}}) = \frac{\varepsilon_{r1}k_o^2\tan\delta_1}{2\beta}\cdot\frac{-bk_{y1}+\sin(bk_{y1})}{D_2} + \frac{\varepsilon_{r2}k_o^2\tan\delta_2}{2\beta}\cdot\frac{\sin(bk_{y1})(k_{y1}/k_{y2})^2}{D_2}. \tag{15}$$

The denominators D_1 and D_2 are defined above and the numerators N_3–N_5 are as follows:

$$N_3 = bk_{y1} + \sin(bk_{y1})\left\{1-(2/\varepsilon_{r1})(k_{y1}/k_0)^2\right\}$$
$$N_4 = -bk_{y1} + \sin(bk_{y1})\left\{1-(2/\varepsilon_{r1})(k_{y1}/k_0)^2\right\}$$
$$N_5 = \sin(bk_{y1})(k_{y1}/k_{y2})^2\left\{1+(2/\varepsilon_{r2})(k_{y2}/k_0)^2\right\}.$$

III. Results and Discussion

To validate the analytical procedure developed for the generalized NRD-guide, a logistic comparison is carried out between the measurements reported by Yoneyama in [8] and our modeling results for the fundamental LSM mode of a conventional NRD-guide. As indicated in Fig. 2, a good agreement is observed between the two independent works.

Let us now examine the transmission losses for both $\mathrm{LSM}_{10}$and LSE_{10} modes with respect to various geometrical parameters. Two critical factors should be considered for that purpose: the maximum frequency at which the NRD-guide is being used and its cutoff. These two endpoints are rather meaningful if the losses are compared over the same frequency bandwidth. Similar cutoff frequencies for the LSM_{10} and LSE_{10} modes are necessary since the attenuation becomes usually very large as the frequency goes down toward the cutoff frequency. The use of different cutoff frequencies would prevent a reasonable comparison for a specific frequency bandwidth because the mode with a higher cutoff frequency (LSM_{10} in this case) would be disadvantaged over the mode with a lower cutoff frequency (LSE_{10}). On the other hand, the frequency bandwidth is usually imposed in the design process.

The dielectric materials for our first analysis of a generalized NRD-guide are selected as $\varepsilon_{r1} = 13$, $\tan\delta_1 = 16 \times 10^{-4}$ (GaAs as in [9]) for the core guide, or region I, and $\varepsilon_{r2} = 9.5$, $\tan\delta_2 = 1.5 \times 10^{-4}$ (alumina as in [9]) for the outer region or region II. For a maximum frequency of 53 GHz (the NRD is designed to have its center frequency at 50 GHz and a bandwidth of at least 2 GHz), the parallel-plate separation (dimension a) is set to 0.92 mm. The width of the core guide (dimension b) is selected to obtain similar cutoff frequencies for the two modes, as well as to respect the predesignated frequency bandwidth. Figs. 3 and 4 are used to determine b. Fig. 3 gives the cutoff frequency of all possible LSM and LSE modes against b. The two first lines on the left side are for the LSE_{10} mode (dashed line) and the LSM_{10} mode (solid line). To permit only the propagation of the fundamental mode (the LSE_{10} or LSM_{10}) at the center frequency of 50 GHz and with the required frequency bandwidth of at least 2 GHz, b has to be chosen between 1.25–2.5 mm. The final choice for b is made on the basis of Fig. 4 in order to maximize the frequency bandwidth, namely, $b = 1.8$ mm for the LSM_{10} mode, yielding a frequency bandwidth of 4.8 GHz, and $b = 1.6$ mm for the LSE_{10} mode, leading to a frequency bandwidth of 5.2 GHz. Such a choice of b also accounts for the similarity of the cutoff frequencies, as shown in Fig. 3. Fig. 5 shows calculated results of the transmission losses for the two fundamental modes. We first notice that the difference of the conduction loss is very small around the frequency band of interest. The difference in total loss resides in the difference of the dielectric losses, which is higher for the

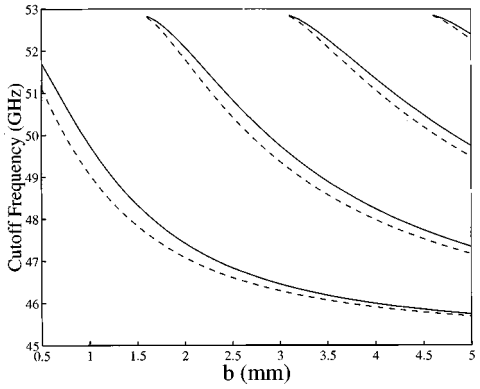

Fig. 3. Cutoff frequencies against width of core dielectric for $a = 0.92$ mm, $\varepsilon_{r1} = 13$, (GaAs), $\varepsilon_{r2} = 9.5$ (Alumina). LSM: solid lines. LSE: dashed lines.

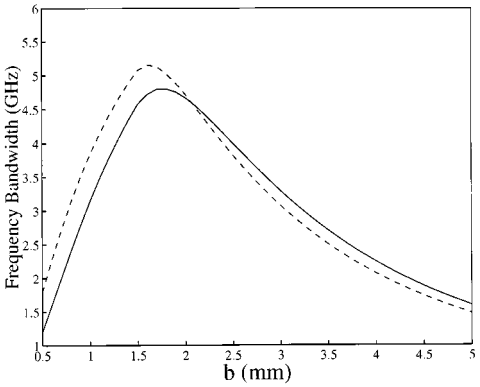

Fig. 4. Frequency bandwidth for $a = 0.92$ mm, $b = 1.8$ mm (LSM) and $b = 1.6$ mm (LSE), $\varepsilon_{r1} = 13$, (GaAs), $\varepsilon_{r2} = 9.5$ (Alumina). LSM: solid line. LSE: dashed line.

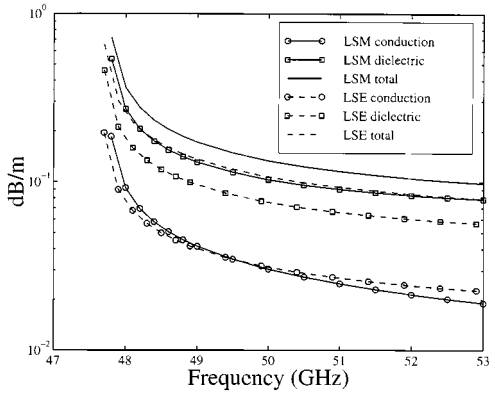

Fig. 5. NRD transmission line losses for $a = 0.92$ mm, $b = 1.8$ mm (LSM) and $b = 1.6$ mm (LSE). Region I (GaAs): $\varepsilon_{r1} = 13$, $\tan\,\delta_1 = 16 \times 10^{-4}$. Region II (Alumina): $\varepsilon_{r2} = 9.5$, $\tan\,\delta_2 = 1.5 \times 10^{-4}$. Metal plates: $\sigma = 6.17 \times 10^7$ S/m.

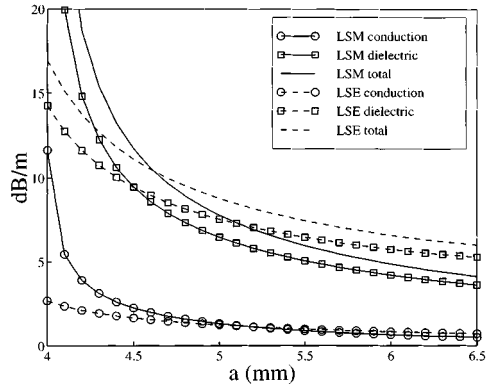

Fig. 6. Transmission loss at center frequency against plate separation for $b = 3.556$ mm, $\varepsilon_{r1} = 2.56$, $\tan\,\delta_1 = 12 \times 10^{-4}$. Metal plates: $\sigma = 3.96 \times 10^7$ S/m. LSM: solid lines. LSE: dashed lines.

LSM_{10} mode. In this case, the LSE_{10} mode seems to be advantageous over the LSM_{10} mode since it is smaller in size with a lower transmission loss as well as a larger frequency bandwidth. Such simple results suggest that the use of LSE mode over its LSM counterpart paid off in some design of the generalized NRD-guide. This is in contradiction as usually perceived in the conventional NRD-guide design.

Figs. 6 and 7 present our calculated results for the transmission loss of an NRD-guide nominally designed for 28 GHz (parallel-plate spacing of 5 mm and core dielectric width of 3.556 mm). Fig. 6 gives the variation of losses versus the parallel-plate spacing, while Fig. 7 gives the variation of losses against the core dielectric strip width. The results presented in these two figures are calculated at the center frequency of the bandwidth, which is defined as $(F_c + F_{\max})/2$ where F_c is cutoff frequency and $F_{\max}$ is given by (1). The center frequency is, therefore, specific for each circuit dimensions. The losses at center frequency as the comparison point between circuits give a meaningful approximation on the average loss of each individual circuit. In Fig. 6, the transmission losses decrease monotonously with an increasing a for both modes. It should be noted that reducing geometrical size of the NRD-guide by using a small plate spacing may be done at the expense of its transmission-loss deterioration. Another interesting behavior is the

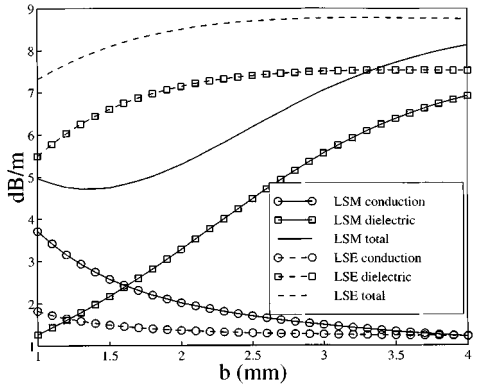

Fig. 7. Transmission loss at center frequency against width of dielectric strip for $a = 5$ mm, $\varepsilon_{r1} = 2.56$, $\tan\,\delta_1 = 12 \times 10^{-4}$. Metal plates: $\sigma = 3.96 \times 10^7$ S/m. LSM: solid lines. LSE: dashed lines.

difference between the transmission losses of the two modes. For the dielectric loss, the LSM mode is better than the LSE mode for a large plate spacing, but the difference between them is reduced as a gets smaller, up to a certain point where the LSE-mode loss become smaller than its LSM counterpart ($a \cong$ 4.5 mm). The total loss behavior is similar to the dielectric loss behavior that becomes dominant as a whole. Both modes present almost the same conduction loss, except that the LSM conduction loss increases faster than its LSE counterpart when a decreases. It is interesting to observe the behavior of conduction and dielectric losses against the width of the core dielectric strip in Fig. 7: the conduction loss decreases while the dielectric loss increases as b increases. Although this trend is true for both modes, the rate of loss variation is different for each of them. The dielectric loss of the LSE mode is much higher than that of the LSM mode, especially when b is small. However, the LSE dielectric loss tends to saturate when b increases up to a certain extent, while the LSM dielectric loss continues to increase. This makes the difference of dielectric loss between the LSE and LSM modes small when b becomes relatively large. The conduction loss behavior is different from the dielectric loss behavior. The LSM mode has a higher conduction loss than the LSE mode. Nevertheless, this LSM conduction loss decreases more rapidly than the LSE mode such that they become equal once b reaches 4 mm. The total transmission loss can be summarized as follows. First, the LSE_{10} mode total loss is higher, but more stable than the LSM_{10} mode over the range of variation of b. Second, the LSM_{10} mode total loss has a minimum point for $b \cong 1.4$ mm, which is rather close to the given value of 1.8 mm. Third, the total losses for the two modes converge to each other as dimension b increases.

IV. Conclusion

Modeling technique for the generalized NRD-guide using closed-form equations is developed for the LSE and LSM modes. Calculated results are verified with measurements reported elsewhere. Our work generates some useful guidelines for the practical NRD-guide design with emphasis on parametric effects on transmission losses caused by imperfect dielectric and metallic materials. It is found that the LSE_{10}

mode can effectively provide a lower transmission loss as compared with its LSM counterpart for a generalized NRD-guide. As indicated in this paper, the use of the LSE mode has several advantages over the LSM mode. It is observed that the losses for the two modes increase monotonously and become comparable as the spacing of the two metallic plates is reduced. However, the loss behaves quite differently as the width of the core dielectric strip increases. The LSE total loss tends to saturate for a large width of the dielectric strip, while the LSM total loss continues to increase and they converge to each other. It is also found that the LSM total loss has a minimum point because its decreasing conduction and increasing dielectric losses share a comparable magnitude.

REFERENCES

[1] T. Yoneyama and S. Nishida, "Non-Radiative dielectric waveguide for millimeter-wave integrated circuits," *IEEE Trans. Microwave Theory Tech.*, vol. MTT-29, pp. 1188–1192, Nov. 1981.

[2] K. Wu, "Hybrid three-dimensional planar/nonplanar circuits for microwave and millimeter-wave applications: The state-of-the-art and challenge," *Facta Univ. (NIS) Series: Electron. Energetics*, vol. 11, no. 1, pp. 87–101, 1998.

[3] K. Wu, J. Dallaire, and F. Boone, "Channelized nonradiative-dielectric (NRD) guide for hybrid and monolithic integration technology," in *1998 Asia–Pacific Microwave Conf.*, Japan, Dec. 8–11, 1998, pp. 265–268.

[4] T. Yoneyama, "Millimeter-wave transmitter and receiver using the nonradiating dielectric waveguide," in *IEEE Int. Microwave Symp. Dig.*, Long Beach, CA, 1989, pp. 1083–1086.

[5] A. Bacha and K. Wu, "LSE-mode balun for hybrid integration of NRD-guide and microstrip line," *IEEE Microwave Guided Wave Lett.*, vol. 8, pp. 199–201, May 1998.

[6] A. Bacha and K. Wu, "Toward an optimum design of NRD-guide and microstrip line transition for hybrid integration technology," *IEEE Microwave Theory Tech.*, vol. 46, pp. 1796–1800, Nov. 1998.

[7] C. A. Balanis, *Advanced Engineering Electromagnetics*, New York: Wiley, 1989.

[8] T. Yoneyama, N. Tozawa, and S. Nishida, "Loss measurements of nonradiative dielectric waveguide," *IEEE Trans. Microwave Theory Tech.*, vol. MTT-32, pp. 943–946, Aug. 1984.

[9] Om. P. Gandhi, *Microwave Engineering and Applications*, New York: Pergamon, 1988.

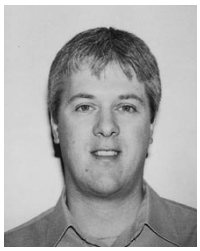

Jean Dallaire (S'96–M'98) was born in Black Lake, P.Q., Canada. He received the B.S and M.Sc.A. degrees in electrical engineering from the École Polytechnique Montréal, Montréal, P.Q., Canada, in 1990 and 1992, respectively, and is currently working toward the Ph.D degree.

From 1992 to 1995, he was with SPAR Aerospace Ltd., Ste-Anne-de-Bellevue, P.Q., Canada, where he was involved with the Transponder/System Group on the MSAT satellite project. He is currently with the Antenna Group, EMS Technologies Canada, Ste-Anne-de-Bellevue, P.Q., Canada, where he is involved in the antenna design for the Skybridge satellite project. His current research interests include electromagnetic fields theory, numerical methods, and leaky-wave NRD-guide feed for antennas.

Ke Wu (M'87–SM'92) was born in Liyang, Jiangsu Province, China. He received the B.Sc. degree with distinction in radio engineering from the Nanjing Institute of Technology (now Southeast University), Nanjing, China, in 1982, and the D.E.A. and Ph.D. degree with distinction in optics, optoelectronics, and microwave engineering from the Institut National Polytechnique de Grenoble (INPG), Grenoble, France, in 1984 and 1987, respectively.

He conducted research in the Laboratoire d'Electromagnetisme, Microondes et Optoelectronics (LEMO), Grenoble, France, prior to joining the Department of Electrical and Computer Engineering, University of Victoria, Victoria, B.C., Canada. Subsequently, he joined the Faculty of Engineering, Department of Electrical and Computer Engineering, École Polytechnique de Montréal, Montréal, P.Q., Canada, as an Assistant Professor, and he is currently a Full Professor. In 1995, he held a Visiting Professorship in France and a 1996–1997 Visiting Professorship at the City University of Hong Kong, as well as several short-term visiting professorships at many other universities. He also holds an Honorary Visiting Professorship at the Southeast University, China. He is currently a guest Professor at the Swiss Federal Institute of Technology (ETH-Zurich), Zurich, Switzerland. He has been the Head of the FCAR Research Group of Quebec on RF and millimeter-wave electronics and the acting Director of the Poly-Grames Research Center. He has authored or co-authored over 245 referred journal and conference papers, and several book chapters. His current research interests involve three-dimensional (3-D) hybrid/monolithic planar and nonplanar integration techniques, active and passive circuits, antenna arrays, advanced field-theory-based computer-aided design (CAD) and modeling techniques, and development of low-cost RF and millimeter-wave transceivers. He is also interested in the modeling and design of microwave photonic circuits and systems. He was Chairperson of the 1996 ANTEM's Publicity Committee and Vice-Chairperson of the Technical Program Committee (TPC) for the 1997 Asia-Pacific Microwave Conference (APMC'97). He has served on the FCAR Grant Selection Committee (1993–1996 and 1998–1999), and the TPC committee for the TELSIKS and ISRAMT. He has also served on the ISRAMT International Advisory Committee. He was the General Co-Chair of the 1999 SPIE's International Symposium on Terahertz and Gigahertz Photonics, Denver, CO. He has served on the editorial and review boards of the *Microwave and Optical Technology Letters.*

Dr. Wu has served on the editorial or review boards of various technical journals, including the IEEE TRANSACTIONS ON MICROWAVE THEORY AND TECHNIQUES, the IEEE TRANSACTIONS ON ANTENNAS AND PROPAGATION, and the IEEE MICROWAVE AND GUIDED WAVE LETTERS. He served on the 1996 IEEE Admission and Advancement (A&A) Committee, the Steering Committee for the 1997 joint IEEE AP-S/URSI International Symposium. He also served as a TPC member for the IEEE MTT-S International Microwave Symposium. He received a URSI Young Scientist Award, the Institute of Electrical Engineers (IEE) Oliver Lodge Premium Award, the Asia-Pacific Microwave Prize Award, the University Research Award "Prix Poly 1873 Pour l'Excellence en Recherche" presented by the École Polytechnique on the occasion of its 125th anniversary, and the Urgel-Archambault Prize (the highest honor) in the field of physical sciences, Mathematics, and Engineering, presented by the French–Canadian Association for the Advancement of Science (ACFAS).